Journal of ELECTRONIC MATERIALS, Vol. 41, No. 8, 2012
DOI: 10.1007/s11664-012-2150-2
© 2012 TMS

Effect of Nitridation on the Regrowth Interface of AlGaN/GaN Structures Grown by Molecular Beam Epitaxy on GaN Templates

YUEN-YEE WONG,[1,4] WEI-CHING HUANG,[1] HAI-DANG TRINH,[1] TSUNG-HSI YANG,[2] JET-RUNG CHANG,[2] MICHEAL CHEN,[3] and EDWARD YI CHANG[1,2]

1.—Department of Materials Science and Engineering, National Chiao Tung University, Hsinchu 30010, Taiwan. 2.—Department of Electronics Engineering, National Chiao Tung University, Hsinchu 30010, Taiwan. 3.—ULVAC Taiwan Inc., 8F., No. 5, Keji Rd., Hsinchu Science Park, Hsinchu 30078, Taiwan. 4.—e-mail: yuenyee98.mse94g@nctu.edu.tw

AlGaN/GaN structures were regrown on GaN templates using plasma-assisted molecular beam epitaxy (PA-MBE). Prior to the regrowth, nitridation was performed using nitrogen plasma in the MBE chamber for different durations (0 min to 30 min). Direct-current measurements on high-electron-mobility transistor devices showed that good pinch-off characteristics and good interdevice isolation were achieved for samples prepared with a 30-min nitridation process. Current–voltage measurements on Schottky barrier diodes also revealed that, for samples prepared without nitridation, the reverse-bias gate leakage current was approximately two orders of magnitudes larger than that of samples prepared with a 30-min nitridation process. The improvement in the electrical properties is a result of contaminant removal at the regrowth interface which may be induced by the etching effect of nitridation.

Key words: AlGaN/GaN, nitridation, regrowth interfaces, molecular beam epitaxy

INTRODUCTION

AlGaN/GaN high-electron-mobility transistors (HEMTs) are excellent candidates for next-generation high-power and high-frequency applications. To be used in these applications, the HEMT devices require high-crystalline-quality and high-resistivity GaN materials. However, due to the lack of a large-size commercial-grade native substrate, GaN materials are usually grown on a foreign substrate such as sapphire, silicon, or silicon carbide. As a result of large lattice and thermal expansion coefficient mismatches between the GaN films and these substrates, high threading dislocation (TD) density is generated in the materials and GaN device performance is degraded. Dislocations are known to reduce the carrier mobility[1–3] and to deteriorate the leakage current[4,5] in GaN devices. Recently, advances in hydride vapor-phase epitaxy[6] and ammonothermal growth[7] methods used to produce high-quality GaN substrates have attracted much attention for direct growth of AlGaN/GaN structures. The homoepitaxial growth has proven useful for achieving AlGaN/GaN structures with better quality[2,8] and less inherent stress compared with those grown on foreign substrates. Despite the improvement in crystal quality, HEMT devices regrown on GaN substrates still suffer from inferior electrical properties. This is due to the presence of a parasitic conduction path at the regrowth interface (RI) of the structure as a result of surface contamination on the GaN substrate after exposure to air.[9,10] The contaminants induce charges at the RI, resulting in poor pinch-off characteristics and poor interdevice isolation of HEMT devices.

(Received January 15, 2012; accepted May 19, 2012; published online June 6, 2012)

Various methods have been proposed to reduce the charges at the RI. These include the polarization and the dopant compensation methods. The former method was achieved by inserting an AlN nucleation layer prior to the MBE regrowth.[11] The AlN layer, with large energy bandgap and polarization dipole, induced band bending and thus formed a large energy barrier between the channel and the RI. On the other hand, the latter method, which is more widely employed, was carried out by introducing an acceptor-doped layer to compensate the n-type doping at the RI. This was achieved by using (i) a regrown C-doped semi-insulating (SI) GaN,[12] (ii) subsurface Fe-doped SI GaN,[10] or (iii) an Fe-doped GaN template followed by ultraviolet photo-enhanced chemical etching of the GaN template.[9] In this work, we reduced the charges at the RI between the AlGaN/GaN structure and the GaN template by using nitrogen plasma treatment, or nitridation. The effects of nitridation time on the electrical and material properties of this structure are also investigated.

EXPERIMENTAL PROCEDURES

Unintentionally doped GaN templates approximately 1.5 μm thick were first prepared on a sapphire substrate using a metalorganic chemical vapor deposition system (MOCVD; EMCORE D-180). In this study, the GaN templates were prepared from the same MOCVD growth run to ensure that they had identical properties. After the growth, the GaN templates were removed from the chamber and left exposed to air for approximately 1 week before regrowth of AlGaN/GaN structures using plasma-assisted molecular beam epitaxy (PA-MBE; ULVAC). In the MBE chamber, the templates were annealed briefly at 800°C (for a few minutes) until the streaky reflection high-energy electron deflection patterns became sharp and bright. Then, the substrate temperature was lowered to 740°C for the regrowth of the AlGaN/GaN structures. Prior to the regrowth, a nitridation process was performed using nitrogen plasma in the MBE chamber. Three samples with 0 min, 15 min, and 30 min nitridation treatment, designated as samples A, B, and C, respectively, were prepared for investigation of the nitridation effect on the RI. During the nitridation process, two plasma generators with power set at 350 W were used to enhance the nitrogen radical supply. After that, an identical AlGaN/GaN structure (25 nm/400 nm) was grown on these templates. The Al composition in the AlGaN layer was approximately 25%. The detailed growth parameters of the AlGaN/GaN material have been described elsewhere.[13] Hall measurement samples, HEMT devices, and Schottky barrier diodes (SBDs) were fabricated to check the electrical properties of the regrown AlGaN/GaN structures. Ohmic contacts to these devices were formed using electron-beam evaporation of a Ti (200 Å)/Al (1200 Å)/Ni (250 Å)/Au (1000 Å) metal stack, followed by 800°C rapid thermal annealing for 1 min. Meanwhile, Schottky contacts were formed by Ni (200 Å)/Au (3000 Å) metal deposition. Hall measurements were performed using the van der Pauw contact configuration. The HEMT devices fabricated in this study had 7-μm source–drain spacing with 2-μm gate length. Mesa isolation was achieved with Cl_2/Ar inductively coupled plasma etching to depth of $\sim$150 nm, which is well below the two-dimensional electron gas (2DEG) channel. The circular SBDs consisted of a Schottky contact with diameter of 50 μm at the center of diode, and an ohmic contact formed as the outer ring. The spacing between the Schottky and ohmic contacts was also 50 μm. For material characterization, high-resolution x-ray diffraction (HRXRD; Bede D1 system) was used to characterize the GaN crystal quality. Meanwhile, time-of-flight secondary-ion mass spectroscopy (SIMS; ION-TOF, TOF.SIMS IV) was used to determine the impurities present in the structure. In addition, atomic force microscopy (AFM; Digital Instrument, D3100) and Auger electron spectroscopy (AES; Microlab 350) were also employed to check the effect of nitridation on the bare GaN template surfaces.

RESULTS AND DISCUSSION

Hall measurement results for AlGaN/GaN structures are presented in Table I. The sheet carrier concentrations (N_s) of samples A and B are much higher than that of sample C. However, from both simulation[14] and experimental[15] results, typical N_s values for similar material structures are always less than 1.5×10^{13} cm^{-2}. This suggests that the excess carriers in samples A and B should be contributed from outside the 2DEG channels. As a result, the electron mobility is also significantly lower for these samples. On the other hand, the Hall result of the sample prepared with a 30-min nitridation process easily corresponds to that of a good-quality AlGaN/GaN structure.

Figure 1 shows the direct-current (DC) measurement results of the HEMT devices. It can be seen

Table I. Hall measurement results of AlGaN/GaN structures prepared with different nitridation times

Sample	Nitridation Time (min)	Sheet Carrier Concentration (cm^{-2})	Mobility (cm^2/V s)
A	0	2.86×10^{13}	422
B	15	2.27×10^{13}	603
C	30	1.26×10^{13}	1130

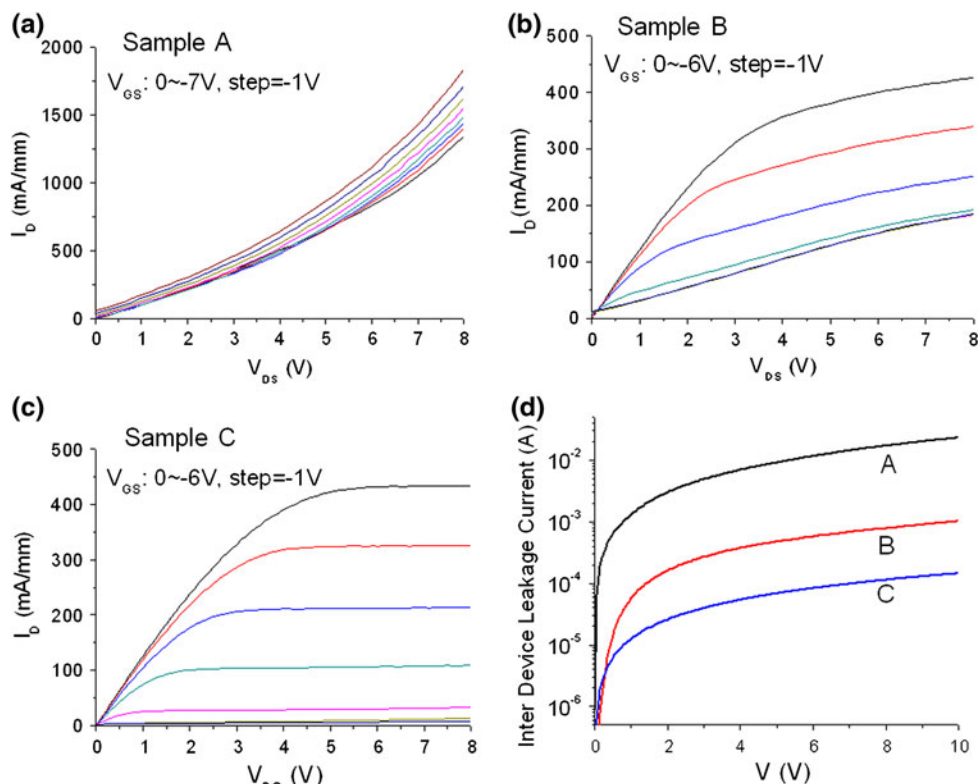

Fig. 1. DC characteristics of HEMT devices prepared with (a) 0 min, (b) 15 min, and (c) 30 min nitridation. (d) The interdevice leakage currents of these samples (color online).

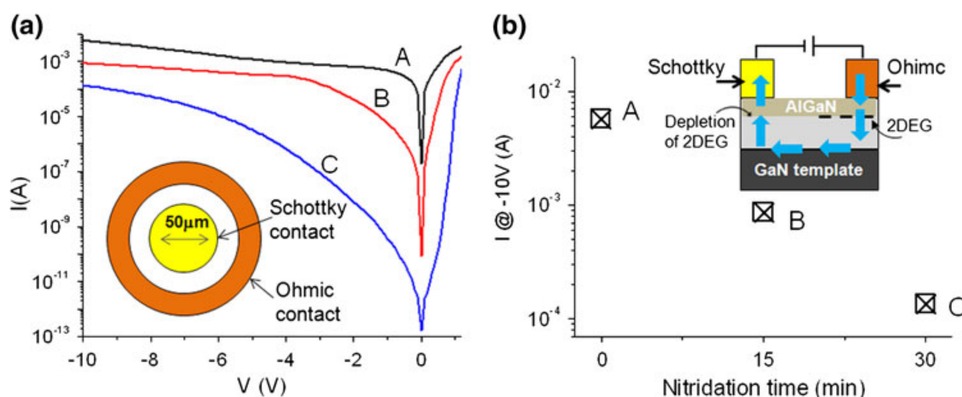

Fig. 2. (a) I–V characteristics of AlGaN/GaN SBDs. The inset illustrates the structure of the SBDs. (b) Reverse-bias leakage currents measured at −10 V. Inset shows the current leaking path in the SBDs (color online).

that the electrical properties of the regrown HEMT structures are sensitively affected by the nitridation time. Figure 1a, b suggests that devices fabricated on both samples A and B had poor electrical properties. Only the sample prepared with a 30-min nitridation process was pinched-off well and had good gate modulation characteristics (Fig. 1c). Further examinations were also carried out to determine the leakage currents at the sample buffers. The buffer leakage currents were measured from the drain pads of two neighboring devices in these samples, and the results are shown in Fig. 1d. Compared with sample C, samples A and B suffered from leaky buffers, which explains the poor performance of the HEMT devices. Both the Hall and DC measurements suggest that parasitic conduction paths are present at the RI of samples A and B.

Large leakage currents were not only observed in the HEMT devices but were also observed in the SBDs fabricated on samples A and B. Figure 2 shows the SBD characteristics of all three samples in this study. The leakage current, measured at 10 V reverse bias, was decreased by approximately two orders of magnitude when the nitridation time

Table II. HRXRD results and SBD characteristics of the samples prepared with different nitridation times

Sample	HRXRD FWHM (arcsec) (002)	HRXRD FWHM (arcsec) (102)	Ideality Factor	SBD's Barrier Height (eV)
A	298	680	4.93	0.36
B	307	673	2.33	0.55
C	310	658	1.36	1.05

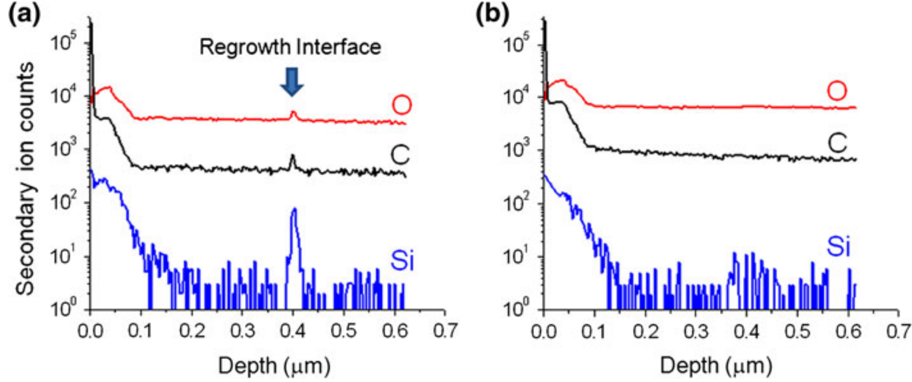

Fig. 3. SIMS results of HEMT structures regrown on samples prepared with (a) 0 min and (b) 30 min of nitridation (color online).

was increased from 0 min to 30 min (Fig. 2b). As illustrated in the inset of Fig. 2b, the leakage current in the SBDs may flow vertically across the AlGaN/GaN structure and laterally across the RI. For GaN materials, TDs, especially screw TDs, are generally known to form the conduction paths for leakage current in the vertical direction.[5,13] To compare the crystal quality of the samples used in this study, HRXRD analyses were performed. The rocking curves (ω scans) for both the GaN symmetric plane (002) and asymmetric plane (102) were scanned, and their full-widths at half-maximum (FWHM) are summarized in Table II. The HRXRD results suggested that all three samples had the same crystal quality, as the FWHM values were similar. This means that the nitridation time did not affect the crystal quality of the regrown GaN materials. Therefore, the improvement of the leakage current by nitridation may be attributed to the increase of the resistivity in both the RI and the TDs. The reason for the increase of resistivity in the TDs will be discussed later.

Meanwhile, from the measurement of the SBD forward currents, the characteristics of the fabricated SBD devices can also be determined. The current density in the forward direction can be expressed using the following equation:[16]

$$\boldsymbol{J} = A^{**}T^2 \exp(-q\phi_b/kT)\exp(qV/nkT), \quad \text{for } V \gg kT/q, \tag{1}$$

where $\boldsymbol{J}$ is the current density, A^{**} is the effective Richardson constant, T is absolute temperature, q is the electron charge, ϕ_b is the barrier height, k is Boltzmann's constant, V is the applied voltage, and n is the ideality factor. In this study, a Richardson constant of 24 was used for the AlGaN layer.[14] The ϕ_b and n values of the samples can therefore be calculated and are listed in Table II. It is shown that the SBD fabricated on sample C had the highest barrier height of 1.05 eV. As the nitridation time decreased, the barrier height decreased, and this explains the large leakage currents for SBDs fabricated on samples A and B. Besides, the SBDs on sample C also had ideality factor of 1.36, which is quite closed to the value of 1 for an ideal SBD. The large leakage current at the Schottky contact can also explain the poor gate control ability observed in the HEMT devices for samples A and B.

To explain the origin of the leakage currents in the HEMT and SBD devices, SIMS analysis was performed to check the unintentional impurities in the samples. Figure 3a shows that the peak concentrations of silicon, oxygen, and carbon were observed at the RI of sample A. These impurities, especially Si and O, are believed to induce parasitic charges at the RI and thus degrade the material electrical properties.[10,11] In contrast, these impurities were effectively reduced by the 30-min nitridation process, as seen in sample C (Fig. 3b).

To gain an insight into the effect of nitridation on the GaN template surface, AFM and AES analyses

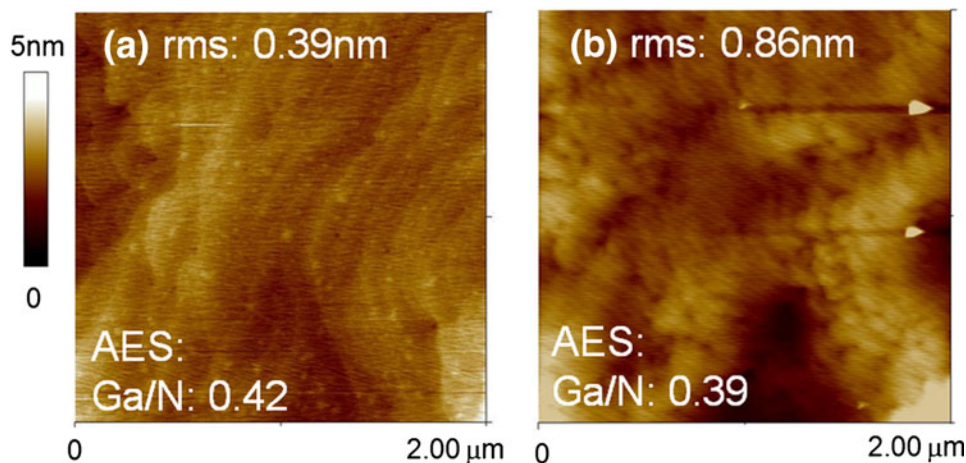

Fig. 4. AFM images of GaN templates after (a) 0 min and (b) 30 min of nitridation. The Ga/N ratios shown in the AFM images were obtained from AES analysis.

were performed. AFM images reveal that the template surface without nitridation (Fig. 4a) is relatively smooth compared with the template surface after a 30-min nitridation process (Fig. 4b). The root-mean-square (rms) roughness of these samples was 0.39 nm and 0.86 nm, respectively. The roughening of the nitridated sample could be induced by the etching effect in the nitrogen plasma. Frayssinet et al.[17] have shown that the GaN film can be etched away slightly in the nitrogen plasma. The etching effect may cause the removal of Si, O, and C impurities at the RI, as determined from the SIMS results. As a result, the parasitic charges at the RI were also reduced. On the other hand, many tiny particles were observed on the GaN template surface without nitridation. To determine the chemical compositions of these particles, the template surfaces were characterized using AES. The surface elements of Ga and N for samples prepared with 0 min and 30 min nitridation were compared, and their ratios are also shown in Fig. 4. AES performed over an area of 10 μm $\times$ 10 μm showed higher Ga/N ratio ($\sim$7%) on the sample surface prepared without nitridation. In a normal growth condition, the difference in Ga/N ratio of these GaN templates (maybe in the form of N-vacancy), which were prepared in the same MOCVD growth run, should be much smaller than 10^{19} cm^{-3} ($\sim$0.1%), well below the detection limit of Auger analysis. So, it is believed that the large difference in Ga/N for different samples was a result of the N_2 plasma treatment. The larger Ga/N ratio found on sample without nitridation implies that the tiny particles observed by AFM are Ga droplets. A small amount of Ga might have resulted from GaN decomposition upon high-temperature annealing in the MBE chamber.[18] The Ga atoms formed into droplets after the sample was cooled. During the regrowth, however, these excess Ga atoms can be incorporated into the screw TDs in the regrown structure and increase the conductivity of the TDs.[19] Therefore, large leakage currents are observed in the fabricated devices, as shown above, even at low bias voltages, due to the formation of low-resistance paths in the vertical direction. This result may explain why *in situ* thermal treatment alone was not sufficient to remove the RI charge.[9] It suffices to say that both the impurities and Ga atoms were removed at the RI after the nitridation and therefore the leakage currents in the devices were reduced. In the presence study, however, it is hard to tell whether the impurities or the Ga atoms contribute more to the leakage current. Additional and careful examinations should be conducted to distinguish these two effects. Besides, more work should also be performed to find an optimum nitridation condition based on the interplay between plasma power, substrate temperature, and nitridation duration.

CONCLUSIONS

The effects of nitridation on GaN templates prior to regrowth of AlGaN/GaN structures by MBE were investigated. AlGaN/GaN HEMTs with good pinch-off characteristics and good interdevice isolation, and SBDs with reduced leakage currents at reverse bias, were fabricated on samples prepared with 30 min of nitridation. From the material analyses, the nitridation process did not affect the crystal quality of the regrown materials but was found to be useful for removing the charges at the RI by removing the impurities, such as Si, O, C, and Ga, on the GaN template surface. The removal of Si, O, and C by nitridation could be attributed to the nitrogen plasma etching process. The nitridation is also believed to have eliminated the excess Ga on the template surface, probably by the formation of new GaN material at the RI. Apparently, the nitridation step used in this study is in contrast to other plasma treatments, such as Ar and He

plasmas, which induce GaN dissociation and generate N-vacancies at the material surface.[20,21] The N-vacancy is generally known as a source of free electrons that increase the conductivity of GaN material.

ACKNOWLEDGEMENTS

This work was supported by the National Science Council of Taiwan under Research Grants NSC 98-2923-E-009-002-MY3. The authors would like to thank ULVAC Taiwan Inc. for MBE maintenance support.

REFERENCES

1. J.H. You, J.-Q. Lu, and H.T. Johnson, *J. Appl. Phys.* 99, 033706 (2006).
2. C. Skierbiszewski, K. Dybko, W. Knap, M. Siekacz, W. Krupczynski, G. Nowak, M. Bockowski, J. Lusakowski, Z.R. Wasilewski, D. Maude, T. Suski, and S. Porowski, *Appl. Phys. Lett.* 86, 102106 (2005).
3. N.G. Weimann, L.F. Eastman, D. Doppalapudi, H.M. Ng, and T.D. Moustakas, *J. Appl. Phys.* 83, 3656 (1998).
4. K.H. Lee, S.J. Chang, P.C. Chang, Y.C. Wang, and C.H. Kuo, *J. Electrochem. Soc.* 155, H716 (2008).
5. J.W.P. Hsu, M.J. Manfra, D.V. Lang, S. Richter, S.N.G. Chu, A.M. Sergent, R.N. Kleiman, L.N. Pfeiffer, and R.J. Molnar, *Appl. Phys. Lett.* 78, 1685 (2001).
6. C.-C. Tsai, C.-S. Chang, and T.-Y. Chen, *Appl. Phys. Lett.* 80, 3718 (2002).
7. T. Hashimoto, F. Wu, J.S. Speck, and S. Nakamura, *Nat. Mater.* 6, 568 (2007).
8. M.J. Manfra, K.W. Baldwin, A.M. Sergent, R.J. Molnar, and J. Caissie, *Appl. Phys. Lett.* 85, 1722 (2004).
9. J.H. Ryou, J.P. Liu, Y. Zhang, C.A. Horne, W. Lee, S.C. Shen, and R.D. Dupuis, *Phys. Status Solidi (c)* 5, 1849 (2008).
10. Y. Cordier, M. Azize, N. Baron, Z. Bougrioua, S. Chenot, O. Tottereau, J. Massies, and P. Gibart, *J. Cryst. Growth* 310, 948 (2008).
11. Y. Cao, T. Zimmermann, H. Xing, and D. Jena, *Appl. Phys. Lett.* 96, 042102 (2010).
12. G. Koblmüller, R.M. Chu, A. Raman, U.K. Mishra, and J.S. Speck, *J. Appl. Phys.* 107, 043527 (2010).
13. Y.-Y. Wong, E.Y. Chang, T.-H. Yang, J.-R. Chang, J.-T. Ku, M.K. Hudait, W.-C. Chou, M. Chen, and K.-L. Lin, *J. Electrochem. Soc.* 157, H746 (2010).
14. N. Zhang, *Electrical and Computer Engineering*, PhD (University of California at Santa Barbara, 2002), p. 155.
15. R. Quay, *Gallium Nitride Electronics* (Germany, Heidelberg: Springer, 2008), pp. 91–138.
16. R. Williams, *Modern GaAs Processing Methods* (Norweed, MA: Artech House, 1990), pp. 241–270.
17. E. Frayssinet, P. Prystawko, M. Leszczynski, J. Domagala, W. Knap, and J.L. Robert, *Phys. Status Solidi (a)* 181, 151 (2000).
18. S. Fernandez-Garrido, G. Koblmuller, E. Calleja, and J.S. Speck, *J. Appl. Phys.* 104, 033541 (2008).
19. J.W.P. Hsu, M.J. Manfra, S.N.G. Chu, C.H. Chen, L.N. Pfeiffer, and R.J. Molnar, *Appl. Phys. Lett.* 78, 3980 (2001).
20. C. Eddy and B. Molnar, *J. Electron. Mater.* 28, 314 (1999).
21. Z.-Q. Fang, D.C. Look, X.-L. Wang, J. Han, F.A. Khan, and I. Adesida, *Appl. Phys. Lett.* 82, 1562 (2003).